# Progress Report 1: Resilience and Adaptation to Climatic Extreme Wildfires (RACE Wildfires)

Ronchi, Enrico; Rohaert, Arthur; Wahlqvist, Jonathan; Wetterberg, Niklas; Intini, Paolo

2022

*Document Version:*
Publisher's PDF, also known as Version of record

Link to publication

*Citation for published version (APA):*
Ronchi, E., Rohaert, A., Wahlqvist, J., Wetterberg, N., & Intini, P. (2022). *Progress Report 1: Resilience and Adaptation to Climatic Extreme Wildfires (RACE Wildfires)*. Lund University, Department of Fire Safety Engineering.

*Total number of authors:*
5

# Progress Report 1: Resilience and Adaptation to Climatic Extreme Wildfires (RACE Wildfires)

Enrico Ronchi

Arthur Rohaert

Jonathan Wahlqvist

Niklas Wetterberg

Paolo Intini

Department of Fire Safety Engineering

Lund University, Sweden

Lund 2022

Report 3248

# Progress Report 1: Resilience and Adaptation to Climatic Extreme Wildfires (RACE Wildfires)

Enrico Ronchi

Arthur Rohaert

Jonathan Wahlqvist

Niklas Wetterberg

Paolo Intini

Lund 2022

# Progress Report 1: Resilience and Adaptation to Climatic Extreme Wildfires (RACE Wildfires)

Enrico Ronchi, Arthur Rohaert, Jonathan Wahlqvist, Niklas Wetterberg, Paolo Intini

**Report** 3248

**ISRN:** LUTVDG/TVBB-3248-SE

**Number of pages**: 33

**Keywords**: wildfires, fire safety, evacuation, smoke, simulation, wildland-urban interface

**Abstract.** This is the first progress report of the international project funded by the National Research Council of Canada called Resilience and Adaptation to Climatic Extreme Wildfires (RACE Wildfires). In this first phase, the research performed included two main tasks: 1) the development of a sub-model for the representation of the impact of reduced visibility conditions on driving speed and 2) the development of a conceptual model for the study of the impact of the pandemic on shelter availability and destination choice. An experimental dataset collected in a virtual reality environment has been used to develop a sub-model for macroscopic traffic models considering the impact of reduced visibility conditions on driving speed. An application of a calibrated traffic model considering the impact of smoke has been performed using the WUI-NITY platform, an open multi-physics platform which includes wildfire spread, pedestrian response and traffic modelling. Verification testing has been performed as well. A conceptual framework for the development of a destination choice model to be applied in wildfire scenarios has also been developed.



| Avdelningen för brandteknik | Department of Fire Safety Engineering |
|---|---|
| Lunds universitet | Lund University |
| P.O. Box 118 | P.O. Box 118 |
| 221 00 Lund | SE-221 00 Lund, Sweden |
| brand@brand.lth.se | brand@brand.lth.se |

## Acknowledgements

The authors wish to acknowledge the support from the Collaborative R&D Initiative of the National Research Council of Canada (grant #STR2-0201) for contributing to funding this research. The authors are also thankful to the National Institute of Standards and Technology for financially contributing to the development of the WUI-NITY tool. The authors wish to acknowledge all collaborators in the RACE Wildfire project.

**Table of Contents**

# Nomenclature

Quantities

| | |
|---|---|
| D | optical density (1/m) |
| k | vehicle density (veh/km/lane) |
| q | traffic flow (veh/h/lane) |
| v | vehicle speed (km/h) |
| a | parameters of the model in the Highway Capacity Manual (exponent calibration parameter) |
| a, b, c | parameters of the model by Van Aerde and Rakha |
| c | parameter of the model by del Castillo and Benítez (km/h) (kinematic wave speed at jam density) |
| α | reduction coefficient of the critical flow for reduced visibility conditions (-) |
| β | reduction coefficient of the free flow speed for reduced visibility conditions (-) |
| γ | reduction coefficient of the critical speed for reduced visibility conditions (-) |
| δ | reduction coefficient of the jam density for reduced visibility conditions (-) |

Subscripts

| | |
|---|---|
| $\square_b$ | quantity $\square$ at the breaking point, where velocity becomes density depended |
| $\square_c$ | quantity $\square$ at peak capacity, critical quantity |
| $\square_f$ | quantity $\square$ in entirely sparse traffic, free-flow situation |
| $\square_j$ | quantity $\square$ in entirely jammed traffic, total congestion |
| $\square_{sm}$ | quantity $\square$ in for reduced visibility conditions |

Units

| | |
|---|---|
| h | hours |
| km | kilometres |
| lane | number of lanes |
| m | metre |
| pce | passenger car equivalents |
| veh | number of vehicles |

# 1. Introduction

This report presents the interim results of the Resilience and Adaptation to Climatic Extreme Wildfires (RACE Wildfires) project, funded by the National Research Council of Canada. The project included different activities, this report being focused on the development of modelling tools to assess community evacuation protocols.

The project was initiated since the propagation of wildfires towards urbanized areas may result in severe negative impacts, including mass evacuations. Fires may occur in Wildland-Urban Interfaces (WUI), where structures and vegetation merge in a wildfire-prone environment (Mell et al., 2010). The National Research Council of Canada (NRCC) and the National Resources Canada (NRCan) identified a clear research need for reducing the impact of WUI fires. This work included the development of a Canadian National Guide for WUI fires (Benichou et al., 2021). In the context of WUI fire evacuation, modelling tools may be helpful to support decisions both at the planning stage as well as during real-time management (Beverly and Bothwell, 2011). Those tools generally include different modelling layers, such as wildfire spread modelling, human response and movement simulations, and traffic evacuation modelling (Ronchi et al., 2019; Ronchi and Gwynne, 2019).

The present report focuses on the traffic evacuation modelling layer. Such tools can be used to investigate what-if scenarios and perform predictions on the time needed to evacuate a given area (Intini et al., 2019). Two main areas have been explored, the study of the influence of wildfire smoke on driving and the impact of a pandemic on destination choice (i.e. destination modelling).

The impact of wildfire smoke on evacuation is a crucial concern since private vehicles are largely used for these types of scenarios (Westhaver, 2017). However, there is a limited number of studies investigating the strategies and solutions for traffic modelling in case of WUI fire evacuations, compared to other hazards such as hurricanes and floods (Dixit and Wolshon, 2014; Kolen and Helsloot, 2012; Lindell et al., 2011; Wilmot and Mei, 2004; S. D. Wong et al., 2020). Recent research attempted to fill this gap by setting the requirements for the coupling of a traffic modelling layer with a wildfire threat (Beloglazov et al., 2016; Cova et al., 2005; Mitchell et al., 2022; Ronchi et al., 2019).

On one hand, fire spread modelling outputs can be used as input for trigger points/buffers (Mitchell et al., 2022) defining the time/location at which different areas should be evacuated (Cova et al., 2005; Li et al., 2015). Those fire spread-dependant trigger models can be integrated with traffic models for simulating the subsequent evacuation stage (Dennison et al., 2007). On the other hand, fire spread can progressively result in the closure of some roadway links, which can no longer be considered for evacuation purposes (Intini et al., 2019; Ronchi et al., 2019; Ronchi and Gwynne, 2019) or affect driving behaviour (Wetterberg et al., 2021). However, the evolution of the fire spread is associated with several uncertainties since it depends on several factors, such as fire, vegetation, topography and environmental variables (Wolshon and Marchive, 2007).

Smoke propagation and associated visibility conditions should be considered explicitly. In fact, while the fire spread or the spotting phenomenon (see e.g., (Tohidi, 2016)) may have not yet caused the complete closure of a roadway link, traffic may be influenced by the presence of smoke (Intini et al., 2019; Wetterberg et al., 2021). In fact, smoke affects visibility and visibility, in turn, may affect driving behaviour, i.e., driving speeds (Wetterberg et al., 2021). Hence, while the coupling of fire models with traffic models may help in identifying the dynamic evolution of the road network available for evacuation, the influence of smoke on driving evacuation behaviour may be even more complex to assess.

Smoke may have a somewhat similar influence on driving behaviour such as adverse weather conditions, which may impair driving performance. However, while rainy and snowy conditions were consistently found to affect traffic flow variables such as speeds and capacity (Dhaliwal et al., 2017; Rakha et al., 2007), there are mixed results for foggy conditions. In fact, these conditions may result in a decrease in speed and capacity (Hoogendoorn et al., 2010), an increase in speed (Snowden et al., 1998), or a decrease in perceived speed as a function of visibility, an effect which can also depend by the simulation environment (Brooks and Rafat, 2015). However, these studies do not reflect evacuation conditions, which may in turn also affect driving behaviour (Wong et al., 2020). In fact, it should be considered that most drivers may be unfamiliar with driving during an evacuation scenario, which can be associated with a decreased speed with respect to familiar environments (Colonna et al., 2016). Moreover, flow capacity drops can also be observed during evacuations (Sullivan et al., 2010). To our knowledge, there are no attempts in previous research at modelling traffic flow relationships in case of reduced visibility conditions due to wildfire smoke, while this could be a clear contribution to the body of research and practice.

In parallel with the development concerning the smoke impact on evacuation, this work includes developments concerning the impact of a concurrent pandemic threat. The Covid19 pandemic has demonstrated the added complexities associated with population safety in case of concurrent threats (Hassan and Mahmoud, 2021; Henderson, 2020; Sugg et al., 2022). Community evacuation plans should take into consideration the concurring effects of a wildfire threat and a disease spread. Existing wildfire evacuation modelling tools do not explicitly account for the impact of a pandemic scenario. This means that there is a dire need to develop a sub-model which can be implemented in evacuation models so that their predictive capabilities are accurate. The Covid19 pandemic has shown that models should take into account issues such as the impact of physical distancing on shelter capacity, occupancy limits and route management. Destination models should explicitly take into account their possibly reduced capacity and the process of providing information to evacuees on shelter availability. This includes representing compliance with the information received concerning transportation modes to shelters, shelter relocations or temporary refuge areas within and outside the affected communities. This may in turn also affect route and destination choices. The combination of those variables, along with the possible impact on the initial response to incident notification needs to be included in existing evacuation modelling tools.

## 1.1 Aim and objectives

This work investigates improvements needed in traffic evacuation modelling tools for wildfire scenarios to improve the accuracy of their results.

The first objective is to study the influence of smoke on driving behaviour during evacuations. Given the difficulty of acquiring actual data during real-world evacuations with the presence of smoke, its influence on driving behaviour may be assessed through simulations, which can provide standardized, easy-to-collect data even for hazardous driving environments which could expose drivers to risks (Kinateder et al., 2014). To date, one study (Wetterberg et al., 2021) evaluated the impact of smoke on driving speeds by performing a virtual reality experiment. This study is used as starting point for the modelling work. The results show that different optical density values due to the simulated smoke were related to a decrease in the average driver speeds. This preliminary result, coupled with previous findings about capacity reduction during adverse visibility conditions e.g., (Hoogendoorn et al., 2010), has been used to build a relationship to be used in traffic modelling. The objective is therefore the development of a sub-model able to represent the reduction in speed as a function of reduced visibility. This would allow a more conservative and realistic approach when considering the presence of smoke from WUI fires on the road network.

The estimated changes in the traffic flow due to wildfire smoke are implemented into an integrated open modelling framework (Ronchi et al., 2020; Wahlqvist et al., 2021) to make it available for any interested parties. Testing of the new sub-model is also performed.

The second objective includes paving the way for the development of a destination model to be used for wildfire evacuation models in which pandemic scenarios may occur. This involves accounting for shelter availability and compliance with instructions provided and the possible impact on the human response to the wildfire event. This is performed by developing a dedicated conceptual framework for destination modelling which includes the concurrent threat of a pandemic and a wildfire scenario.

## 1.2 Report overview

The first chapter of this report introduces the project, the overall aim and objectives and the report structure. Chapter 2 presents the method employed for the development and implementation of the sub-models for wildfire evacuation simulations. Chapter 3 presents a brief overview of existing approaches adopted for traffic evacuation modelling, particularly focusing on the calibration efforts required for the representation of the impact of smoke on driving. Chapter 4 introduces a conceptual framework for destination modelling considering the impact of a pandemic on traffic evacuation (this includes shelter availability, human response and compliance with instructions received). Chapter 5 presents a general discussion on the sub-models developed and further steps needed for their full implementation in existing multi-physics wildfire evacuation modelling tools.

# 2 Modelling driving speed in smoke

This section introduces a set of mathematical models concerning traffic evacuation simulations adopted for the development of the sub-model considering the impact of smoke on driving speed during wildfire evacuations. As the main focus of this report is macroscopic traffic modelling, only the representation of the fundamental traffic dynamics at the macroscopic level is discussed.

This work makes use of a set of commonly used relationships between speed, flow, and density. The work has been done considering the relationships included in the multi-physics WUI-NITY tool (Ronchi et al., 2020; Wahlqvist et al., 2021), and other macroscopic models which may be suitable for the implementation of the impact of smoke on speed.

## 2.1 Macroscopic traffic models

First, a set of well-known macroscopic traffic models (See Equation 1 to Equation 7) are presented. Those models are relationships which consider the fundamental variables of traffic (e.g. vehicle speed, vehicle density and vehicle flow) for the representation of uninterrupted facilities (e.g. where road links can be assumed unaffected by the presence of intersections for a significant length).

Equation 1 presents the parabolic model by Greenshield (1935), often also referred to as the Lighthill-Whitham-Richards (LWR) model (Lighthill and Whitham, 1955; Richards, 1956).

$$v = v_f \left(1 - \frac{k}{k_j}\right) \qquad \text{[Equation 1]}$$

Equation 2 presents the exponential model by Underwood (1961).

$$v = v_f e^{\left(-\frac{k}{k_c}\right)} \qquad \text{[Equation 2]}$$

Equation 3 presents the North-Western model by Drake et al. (1965).

$$v = v_f e^{\left(-\frac{1}{2}\left(\frac{k}{k_c}\right)^2\right)} \qquad \text{[Equation 3]}$$

Equation 4 presents the bi-linear (triangular) model by Daganzo (1994).

$$v = \begin{cases} v_f, & 0 \le k \le k_c \\ \frac{q_c}{k}\left(\frac{k_j - k}{k_j - k_c}\right), & k_c \le k \le k_j \end{cases} \qquad \text{[Equation 4]}$$

Equation 5 presents the model by Van Aerde and Rakha (Van Aerde and Rakha, 1995; Wu and Rakha, 2009).

$$k = \frac{1}{a + \frac{b}{v_f - v} + c\,v} \; with \begin{Bmatrix} a = \frac{v_f(2v_c - v_f)}{k_j v_c^2} \\ b = \frac{v_f(v_c - v_f)^2}{k_j v_c^2} \\ c = \frac{1}{v_c k_c} - \frac{v_f}{k_j v_c^2} \end{Bmatrix} \qquad \text{[Equation 5]}$$

Equation 6 presents the model by del Castillo and Benítez (1995).

$$v = v_f\left(1 - e^{\left(\frac{c}{vf}\left(1-\frac{k_j}{k}\right)\right)}\right) \qquad \text{[Equation 6]}$$

Equation 7 presents the model available in the Highway Capacity Manual (HCM) (Transportation Research Board and National Research Council, 2016).

$$v = \begin{cases} v_f, & 0 \leq q \leq q_b \\ v_f - \left(v_f - v_c\right)\left(\frac{q-q_b}{q_c-q_b}\right)^a, & q_b \leq q \leq q_c \\ \frac{q_c}{k_j}\frac{q}{q_c-q}, & k_c \leq k \leq k_j \end{cases} \qquad \text{[Equation 7]}$$

In all those models, the traffic density $k$, the speed $v$ and the flow $q = kv$ are the variables and all other quantities are constant parameters (which differ for each road type and each scenario). The first five models (Greenshield (1935), Underwood (1961), Drake et al. (1965), Daganzo (1994), and Van Aerde and Rakha (1995)) rely on parameters that can be physically observed during experiments or measurements by measuring the speed, density and flow:

- $v_f$ speed at entirely sparse traffic, free-flow speed (km/h or mi/h)
- $v_c$ speed at peak capacity, critical speed (km/h or mi/h)
- $q_c$ flow at peak capacity, critical flow, capacity (veh/h/lane)
- $k_c$ density at peak capacity, critical density (veh/km/lane or veh/mi/lane)
- $k_j$ density at entirely jammed traffic, jam density (veh/km/lane or veh/mi/lane)

Based on the macroscopic models presented here, the work was then conducted in two phases. In the first phase, two macroscopic traffic models which were originally adopted (or planned for adoption) by WUI-NITY (Greenshields and Van Aerde & Rakha models respectively) have been re-calibrated to account for the impact of smoke on driving.

In the following phase of the project, traffic evacuation data became available (Ronchi et al., 2021), thus the two models which have shown the greatest fit with traffic evacuation data were used for representing the impact of smoke on driving (Van Aerde & Rakha and Daganzo models). This included a re-calibration of the models and an updated relationship of the impact of smoke on driving speed. In fact, the models by Daganzo (1994) and by Van Aerde and Rakha (1995) seem to fit well to empirical data related to routine traffic and wildfire evacuations (Rohaert et al., 2022). These two models also show trends that are very similar to the model proposed in the Highway Capacity Manual, when using the same parameters (see Figure 1).

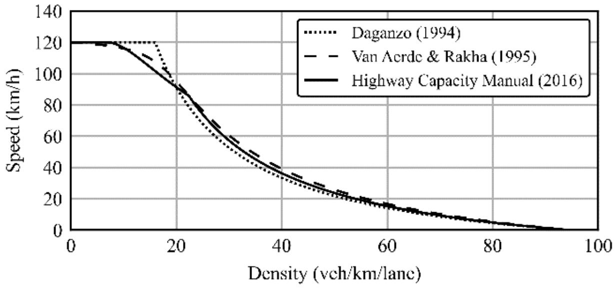


*Figure 1. An example of the Daganzo model, the Van Aerde and Rakha model and the HCM model for a freeway with a speed limit of 120 km/h. The same parameters have been used for all models.*

## 2.2 Reduction factors for the model parameters

The methods section has introduced different models that are used to represent routine traffic at a macroscopic level. However, the parameters present in those models need to be adjusted to model the specific driving behaviour during wildfire evacuations (Ronchi et al., 2021).

Even when there is no smoke present on the road, traffic dynamics during evacuation scenarios seem to be different from those during routine scenarios. Rohaert et al. (2022) sourced traffic flow data from before and during the 2019 Kincade Fire from the Performance Measurement System of the California Department of Transportation and concluded that the evacuation speeds were lower than the routine speeds for mid to high-density traffic while little difference was present for low-density traffic (see Figure 2).

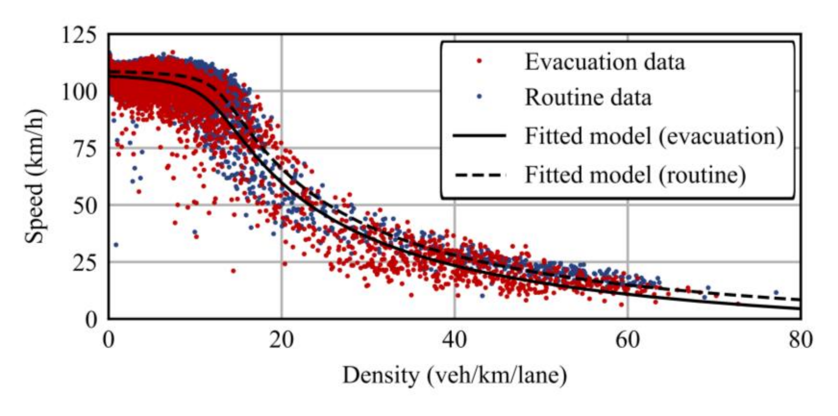


*Figure 2. Van Aerde and Rakha (1995) fitted to the evacuation data and the routine data from the 2019 Kincade Fire (Rohaert et al., 2022).*

At free flow, the speed is barely influenced (reduced by 1.8%). However, the reduction becomes more significant for higher densities. As the density and the speed at capacity dropped by 0.8 and 8.2% respectively, the capacity of the road was reduced by 9.0%. Similarly, Dixit and Wolshon (2014) found capacity reductions of 10% for non-urban areas and 15% for urban areas during hurricane evacuations.

### 2.2.1 Reductions due to adverse weather conditions

Moreover, the reduced visibility, due to the spread of smoke, can further reduce the speed and flow. Under these conditions, the following correction factors can be applied (Equations 8-11):

$$q_{c,sm} = \alpha\, q_c \qquad \text{[Equation 8]}$$
$$v_{f,sm} = \beta\, v_f \qquad \text{[Equation 9]}$$
$$v_{c,sm} = \gamma\, v_c \qquad \text{[Equation 10]}$$
$$k_{j,sm} = \delta\, k_j \qquad \text{[Equation 11]}$$

As mentioned before, many studies have been performed on the effect of adverse weather conditions such as rain and snow on traffic dynamics. A summary of these studies is provided in Table 1. Usually, these studies express the effect through correction factors ($\alpha$, $\beta$, $\gamma$, $\delta$) or reductions ($1-\alpha$, $1-\beta$, $1-\gamma$, $1-\delta$) that can be applied to the parameters that define the macroscopic models.

*Table 1. Reduction factors expressed as percentages for adverse weather conditions.*

| Weather | Location | $1-\alpha$ (%) | $1-\beta$ (%) | $1-\gamma$ (%) | Reference |
|---|---|---|---|---|---|
| Light rain | Los Angeles, CA, USA | 8.65 | 5.7 | 6.91 | (Dhaliwal et al., 2017) |
| Medium rain | Los Angeles, CA, USA | 17.4 | 11.71 | 12.34 | (Dhaliwal et al., 2017) |
| Heavy rain | Los Angeles, CA, USA | 15.34 | 10.22 | 11.85 | (Dhaliwal et al., 2017) |
| Light rain | Multiple locations, USA | 10 - 11 | 2 - 3.6 | 8 - 10 | (Rakha et al., 2007) |
| Heavy rain | Multiple locations, USA | 10 - 11 | 6 - 9 | 8 - 14 | (Rakha et al., 2007) |
| Light snow | Multiple locations, USA | 5 - 16 | 5 - 16 | 12 - 20 | (Rakha et al., 2007) |
| Light rain | Paris, France | 18.5 | 8 | 26 | (Billot et al., 2009) |
| Medium rain | Paris, France | 21 | 12.6 | 40 | (Billot et al., 2009) |
| Trace rain | Minneapolis, MN, USA | 1 - 3 | 1 - 3 | - | (Agarwal et al., 2006) |
| Light rain | Minneapolis, MN, USA | 5 - 10 | 5 - 10 | - | (Agarwal et al., 2006) |
| Heavy rain | Minneapolis, MN, USA | 10 - 17 | 10 - 17 | - | (Agarwal et al., 2006) |
| Trace snow | Minneapolis, MN, USA | 3 - 5 | 3 - 5 | - | (Agarwal et al., 2006) |
| Light snow | Minneapolis, MN, USA | 6 - 11 | 7 - 9 | - | (Agarwal et al., 2006) |
| Heavy snow | Minneapolis, MN, USA | 7 - 13 | 8 - 10 | - | (Agarwal et al., 2006) |
| Reduced visibility | Minneapolis, MN, USA | 10 - 12 | 6.63 - 11.78 | - | (Agarwal et al., 2006) |
| Wet | New England, USA | 0.0 | 8.9 | - | (Agbolosu-Amison et al., 2004) |
| Wet & snowy | New England, USA | 5.3 | 10.7 | - | (Agbolosu-Amison et al., 2004) |
| Wet & slushy | New England, USA | 14.3 | 23.2 | - | (Agbolosu-Amison et al., 2004) |
| Slushy in wheel | New England, USA | 21.7 | 28.6 | - | (Agbolosu-Amison et al., 2004) |
| Snowy & sticky | New England, USA | 18.2 | 33.9 | - | (Agbolosu-Amison et al., 2004) |
| Light rain | Hampton Roads, VA, | 4 - 10 | 5 - 6.5 | - | (Smith et al., 2004) |
| Heavy rain | Hampton Roads, VA, | 25 - 30 | 5 - 6.5 | - | (Smith et al., 2004) |
| Light rain | Mississauga, ON, | 0 | 1.9 | 7.9 - 13.7 | (Ibrahim and Hall, 1994) |
| Heavy rain | Mississauga, ON, | 14 - 15 | 4.8 - 6.7 | 14.6 - 16.8 | (Ibrahim and Hall, 1994) |

Only a few studies mention the reduction of the jam density ($\delta$). Rakha et al. (2007) that the reduction is non-significant ($\delta \approx 1$). The same conclusion can be drawn from the study by Billot et al. (2009). Moreover, the jam density is considered constant in the Highway Capacity Manual

(2016, exhibit 12.7 and 12.8). No studies have been found that contradict this assumption. Consequently, the same assumption has been made in this report for driving through smoke.

### 2.2.2 Reductions due to wildfire smoke

The only empirical data that is available concerning the reduction factors under reduced visibility conditions due to smoke, was obtained by Wetterberg et al. (2021). In the virtual-reality experiment, 46 participants drove on an empty road under five different conditions (see Table 2).

*Table 2: Free flow speed reduction factors as a function of the optical density. Data from Wetterberg et al. (2021)*

| Smoke density | Optical density $D$ [m$^{-1}$] | Free flow speed reduction $\beta$ (-) |
|---|---|---|
| none | 0.00 | 1.00 |
| low | 0.05 | 0.65 |
| medium | 0.10 | 0.47 |
| high | 0.15 | 0.38 |
| very high | 0.20 | 0.31 |

Wetterberg et al. (2021) proposed a third-degree polynomial to obtain values for the reduction factor $\beta$ as a function of the optical density $D$ (Equation 12).

$$1 - \beta = -101.57D^3 + 49.43D^2 - 9.28D \quad \text{[Equation 12]}$$

However, Equation 12 can be substituted with a simpler power model (with comparable goodness of fit), which does not have any points of inflection (see Equation 13).

$$1 - \beta = 1.474\ D^{0.4594} \quad \text{[Equation 13]}$$

The experimental data, as well as Equation 12 and Equation 13 are shown in the figure below (Figure 3).

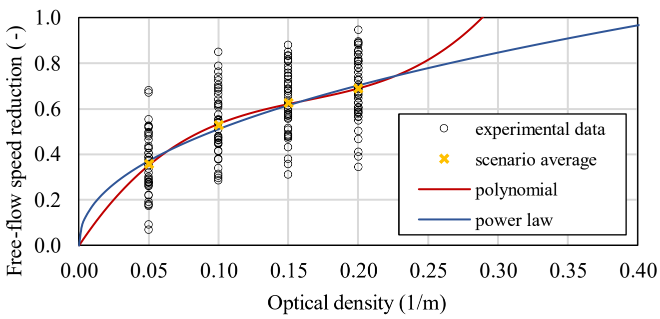


*Figure 3. Relationship between the reduction factor and the visibility. Data from (Wetterberg et al., 2021).*

## 2.3 First calibration of the macroscopic model in WUI-NITY

In this section, the Van Aerde & Rakha model (indicated as VA) and the Greenshields model (indicated as GS) are calibrated for reduced visibility conditions. Further details on this work can be found in the scientific paper associated with this work (Intini et al., 2022).

In the first phase, the reduction factor $\beta$ as a function of the optical density was adopted from the work by Wetterberg et al. (2021), also discussed above. Thereafter, the other factors $\alpha, \gamma, \delta$ were estimated from literature studies (the two first references in Table 1: Rakha et al. (2007) and Dhaliwal et al. (2017)). This resulted in the following assumptions:

$$\begin{cases} \alpha = \gamma = 0.94\,\beta \\ \delta = 1 \end{cases} \quad \text{[Equation 14]}$$

In the studies that were used to derive these relationships between $\alpha$, $\beta$ and $\gamma$, the value of $\beta$ did not decrease below 0.88 while it can drop till 0.31 when driving in smoke (Table 2). Below, we propose different relationships, based on more data. Nevertheless, it should be noted that the second attempt to calibrate macroscopic traffic models would need further developments based on dedicated data collection efforts.

### 2.3.1 Adaptation of the Van Aerde model

To adapt the Van Aerde model, Equation 5 if given explicitly in terms of the parameters in Equation 8 till equation 11:

$$k = \frac{1}{\frac{v_f (v_C - v)^2}{k_j {v_C}^2 (v_f - v)} + \frac{1}{q_C}} \quad \text{[Equation 15]}$$

Next, Equation 8 till Equation 11 and Equation 114 are applied to obtain the adapted VA model, considering reduced visibility conditions (Equation 16).

$$k_{sm} = \frac{1}{\frac{\beta\, v_f\, (\gamma\, v_C - v)^2}{\delta\, k_j\, \gamma^2\, {v_C}^2\, (\,\beta\, v_f - v)} + \frac{1}{\alpha\, q_C}} = \frac{0.94}{\frac{v_f\, (0.94\,\beta\, v_C - v)^2}{0.94\;\beta\, k_j {v_C}^2\, (\beta\, v_f - v)} + \frac{v}{\beta\, q_C}} \quad \text{[Equation 16]}$$

### 2.3.2 Adaptation of the Greenshield model

Analogically, the Greenshield model can be adapted. However, this model relies only on two parameters. Consequently, two of the four correction factors are defined by the other two. The critical speed always equals half of the free-flow speed in this model, which means that the model imposes that $\gamma$ equals $\beta$. Moreover, it imposes that $\alpha$ equals $\gamma\delta$ as the critical density is always half of the jam density. The adjusted Greenshields model is presented in Equation 17.

$$k_{sm} = \delta k_j \left(1 - \frac{v}{\beta\, v_f}\right) = k_j \left(1 - \frac{v}{\beta\, v_f}\right) \quad \text{[Equation 17]}$$

### 2.3.3 An example of the adapted models

The two adapted models are illustrated the five scenarios of the study by Wetterberg et al. (2021), also given in Table 2. The scenarios are applied to a road segment similar to the one in the experiments:

$v_f = 72.4\ \mathrm{km/h}$ (a measurement of the experiment)
$v_c = 36.2\ km/h$ (a reasonable assumption, required for the Van Aerde model)
$q_c = 1300\ veh/h/lane$ (a reasonable assumption, required for the Van Aerde model)
$k_j = 71.8\ veh/km/lane$ (a reasonable assumption, required for both model)

The value of the capacity is suggested in the Planning and Preliminary Engineering Applications Guide to the Highway Capacity Manual (Dowling et al., 2016) for minor two-lane highways with a similar free flow speed. The value for the critical speed is the design value for these two-lane highways according to the HCM (2016). Following these assumptions, the jam density was assumed to be twice the critical density (which is the ratio of the critical flow and the critical velocity). The result is shown in Figure 4 and Figure 5.

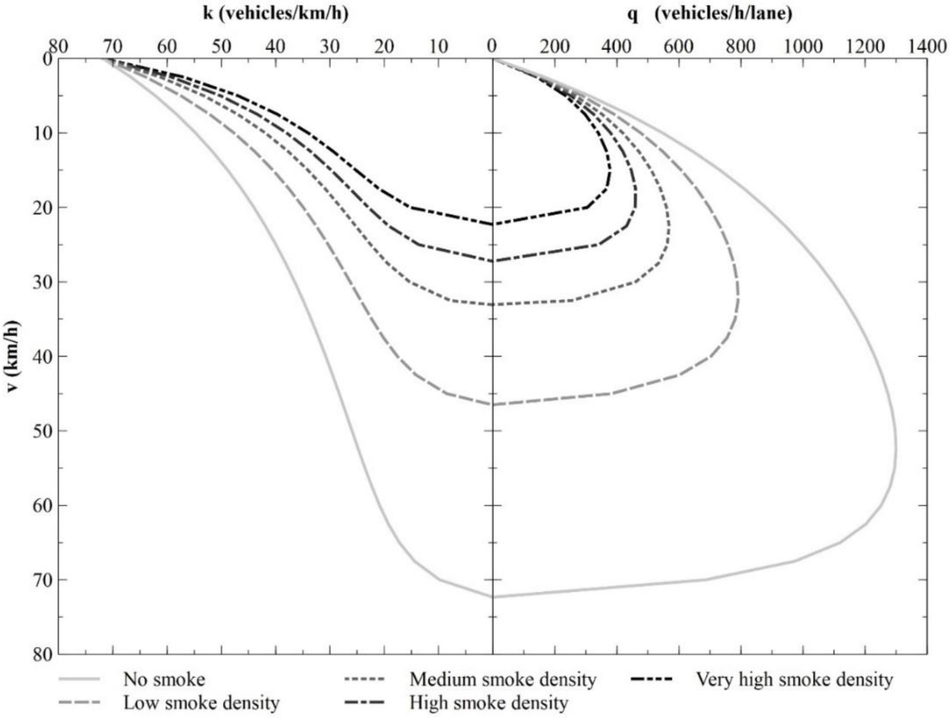


*Figure 4. Diagram of the adapted VA model in different visibility conditions*

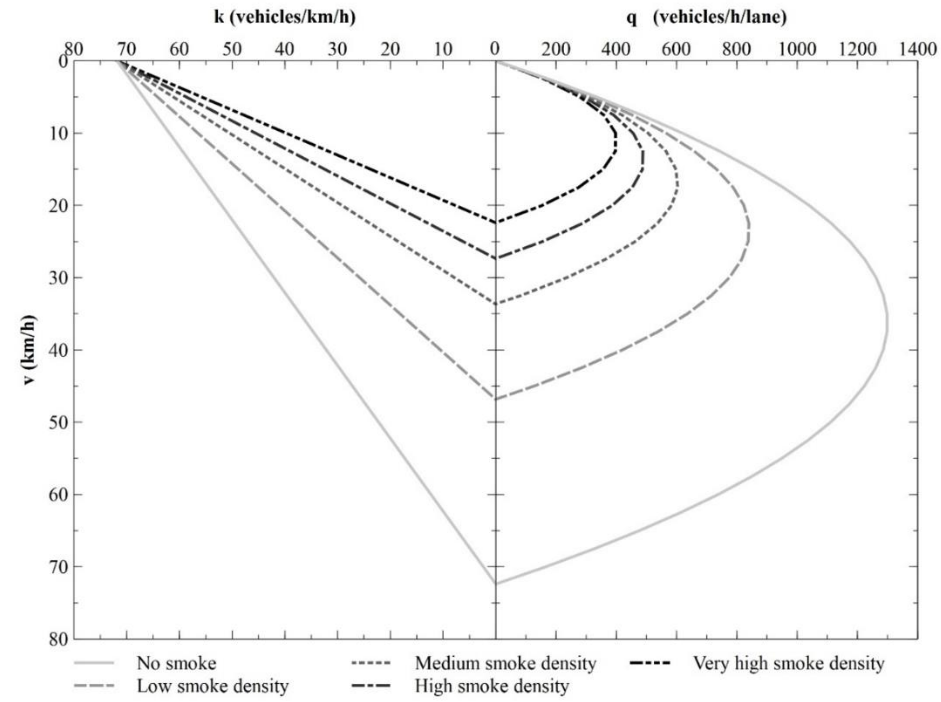


*Figure 5. Diagram of the adapted GS model in different visibility conditions*

### 2.3.4 Implementation and verification of the adapted models

The calibrated model considering the presence of smoke is demonstrated through its implementation in a freely accessibly platform, namely WUI-NITY (Ronchi et al., 2020; Wahlqvist et al., 2021).

The WUI-NITY platform is based on the game engine Unity 3D (Unity Technologies, San Francisco CA, USA) with built-in Virtual Reality (VR) capability acting as a host for different modelling sub-components. In fact, WUI-NITY allows the coupling of the following three modelling layers: (1) a fire spread model; (2) a pedestrian response and movement model; and (3) a traffic model.

The platform is intended as model agnostic to allow the implementation of different modelling tools for each modelling layer depending on the given intended application. In its first implementation, the tool includes macroscopic sub-models for all three modelling layers.

Given the exemplary scope of this platform, a simple macroscopic traffic model (the GS model) was used to represent the traffic evacuation on the egress routes, neglecting the influence of delays at intersections. This is deemed a reasonable assumption for this application as queuing on segments is predominant in the case of large-scale evacuation. In addition, intersections could be operated differently during evacuation (e.g., turning off traffic signals), thus reducing their impact on evacuation time.

In particular, the GS traffic model is implemented in WUI-NITY using a time-step discretisation, as shown in Equation 18.

$$k_j(T+1) = k_j(T) + \frac{\Delta t}{L_j n_j}\left(q_{j,IN}(T) - q_{j,OUT}(T)\right) \qquad \text{[Equation 11]}$$

where:

- $k_j(T)$ is the average traffic density in the road section *j* at the time *T* (vehicles/km/lane);
- $\Delta t = (T+1) - (T)$ is the time step (s), set by default as equal to 1 s;
- $L_j$ is the length of the road section (km);
- $n_j$ is the number of lanes;
- $q_{j,IN}(T)$ is the traffic flow entering the section *j* at the time *T* (vehicles/hour/lane);
- $q_{j,OUT}(T)$ is the traffic flow exiting the section *j* at the time *T* (vehicles/hour/lane).

The main outputs of the traffic simulation for each time step are the number of vehicles which arrive at the destination or in the road network, the vehicular density, the evacuation time curves at each destination and the number of residents, evacuees and those who reach shelters.

Given the functionalities offered by WUI-NITY, a set of verification tests was developed and run to perform an implementation of the developed sub-model in reduced visibility conditions (Ronchi et al., 2021). This verification test is an ideal scenario designed to investigate the current and any future implementation of sub-models concerning driving speed in reduced visibility conditions. The structure and format of the test are in line with the existing verification and validation adopted for evacuation models adopted in building fire safety engineering applications (International Standards Organization, 2020).

The test was run by focusing on the implementation of the adapted Greenshield model in the traffic simulation layer of the WUI-NITY platform. In this example, a single carriageway road (having a speed limit equal to 70 km/h) was considered, by allowing the traffic to move on a single lane for a total length of 1 km (see Figure 6). In this scenario, one vehicle travelling at the assigned maximum speed corresponding to the speed limit (70 km/h) was made to move along the road (from start to destination), with a given set visibility value. The test was repeated by varying the initial vehicular density on the road (e.g. using 5 different levels of vehicular density from the isolated vehicle scenario to the stopped traffic condition, which for this scenario was equal to 75 veh/km/lane) and the visibility (scenarios of Table 2). This allowed testing the competing impact of traffic density and reduced visibility conditions on traffic flow.

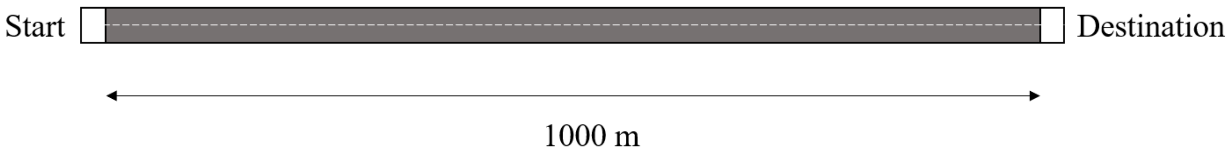


*Figure 6. Geometrical configuration of the verification test*

The following assumptions were adopted while performing the test:

- The Greenshield model was implemented considering a user defined minimum speed to avoid complete congestion. Here, the default 5 km/h was used.
- The given optical density is here assumed uniform across the whole road segment.
- Using an agent-based modelling approach, an IF condition was set up so that when the two concurring variables causing speed reduction would occur (e.g., traffic density and reduced visibility), the minimum speed adopted would be based on the minimum speed driven by the visibility variable rather than the minimum speed due to traffic density (e.g., 1 km/h in this example). This issue has been widely investigated in other evacuation contexts (Ronchi et al., 2013).
- The time step adopted in the calculation was equal to 1s.

As a result of the test, the simulation results were compared to the hand calculations, reported in Table 3.

Please notice that the calculated evacuation times at a density equal to 75 vehicles/km/lane always correspond to 3600 given the assumptions made on minimum speed. The differences between simulated and calculated times were all below 3.3%. In particular, the stall speed was approximated to 1.08 km/h in WUI-NITY rather than the 1 km/h adopted in the hand calculations. The long runtime at the highest vehicle density level makes this small difference in assumed speed more visible. The overall difference in results is caused by the approximation of the speed-density relationship equation implemented in the simulator and hand calculations.

*Table 3. Comparison of calculated and simulated evacuation times*

| | Traffic density (Veh/km/lane) | Evacuation times (s) by smoke density | | | |
|---|---|---|---|---|---|
| | | Low | Moderate | High | Very high |
| Calculation | 1 | 81 | 112 | 138 | 168 |
| Simulation | | 80 | 112 | 137 | 168 |
| Relative difference | | 1.2% | 0% | 0.7% | 0% |
| Calculation | 19 | 106 | 147 | 180 | 219 |
| Simulation | | 105 | 146 | 179 | 219 |
| Relative difference | | 0.9% | 0.7% | 0.6% | 0% |
| Calculation | 38 | 158 | 217 | 265 | 322 |
| Simulation | | 157 | 217 | 265 | 321 |
| Relative difference | | 0.6% | 0% | 0% | 0.3% |
| Calculation | 56 | 295 | 400 | 483 | 577 |
| Simulation | | 294 | 399 | 482 | 576 |
| Relative difference | | 0.3% | 0.2% | 0.2% | 0.2% |
| Calculation | 75 | 3600 | 3600 | 3600 | 3600 |
| Simulation | | 3479 | 3514 | 3530 | 3544 |
| Relative difference | | 3.3% | 2.4% | 1.9% | 1.6% |

## 2.4 Second calibration of the macroscopic model

Based on the experiment by Wetterberg et al. (2021), the first part of the work presented in this report included adjusting the model by Greenshields (1935) and the model by Van Aerde and Rakha (1995) to different optical densities. To do so, $\alpha = \gamma = 0.94\,\beta$ and $\delta = 1$ was assumed. This means that there will be a reduction of the critical velocity and critical flow, even when there is no smoke present ($1 - \alpha = 1 - \gamma = 6\%$ for $D = 0$). Moreover, the relationship between $\alpha, \beta$ and $\gamma$ is based on observed trends for rain and snow, with reduction equal to or smaller than 12%. Note that this relationship has been extrapolated till reduction up to about 70% ($D$ = 0.20 m$^{-1}$).

The assumptions for the correction factors can be considered further. This is a necessary step for their implementation in existing macroscopic traffic models (Greenshields, Daganzo and Van Aerde).

Figure 7 displays the reductions (1 – $\alpha$) as a function of (1 – $\beta$) for all data found in Table 1. When a study reports about an interval, the midpoint is displayed. Figure 7 reveals a positive correlation of medium strength (the sample Pearson correlation coefficient equals 0.473).

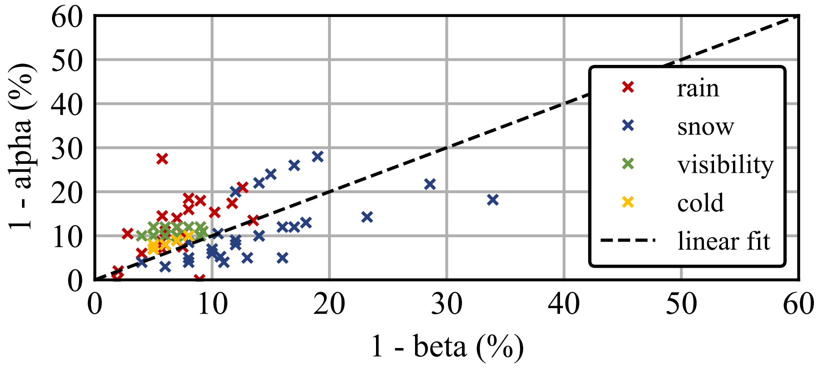


*Figure 7. Relationship between $\alpha$ and $\beta$ based on the data from Table 1.*

Subsequently, a linear fit has been made to describe the relationship (also shown in Figure 7). The fit is forced to intercept the origin ($1-\alpha$ equals 0 when $1-\beta$ does, or in other words, $\alpha$ equals 1 when $\beta$ does). The result is presented in Equation 19.

$$(1-\alpha) = 1.004\,(1-\beta) \rightarrow \alpha \approx \beta \qquad \text{[Equation 19]}$$

Furthermore, it is assumed that the reduction in critical velocity equals the reduction in critical flow ($\alpha \approx \gamma$), just as in the HCM (2016, exhibit 12.7 and 12.8), which means that the critical density is not influenced by the reduced visibility. The jam density is also assumed to be independent of visibility. When employing the power law relation between $\beta$ and $D$, the proposed model can be summarised as in Equation 20.

$$\alpha = \beta = \gamma = 1 - 1.474\,D^{0.4594}, \qquad \delta = 1 \qquad \text{[Equation 20]}$$

As the critical density and the jam density are not affected by the visibility, models can be downscaled linearly to adjust for reduced visibility. The resulting re-calibrated models of Greenshields, Daganzo and Van Aerde & Rakha are presented in the next sections.

### 2.4.1 Calibrated Greenshields model (1935)

The parabolic model by Greenshields (see Equation 1) relies on two parameters: the free-flow speed and the jam density. Consequently, two of the four correction factors are defined by the other two. The critical speed always equals half of the free-flow speed in this model, which means that the model imposes that $\gamma$ equals $\beta$. Moreover, it imposes that $\alpha$ equals $\gamma\delta$ as the critical density is always half of the jam density. The Greenshield model can be adjusted according to Equation 20, as presented in Equation 21.

$$v_{sm} = \alpha\, v_f \left(1 - \frac{k}{k_j}\right) = \alpha\, v \qquad \text{[Equation 21]}$$

Figure 8 shows the calibrated model for five different visibility scenarios.

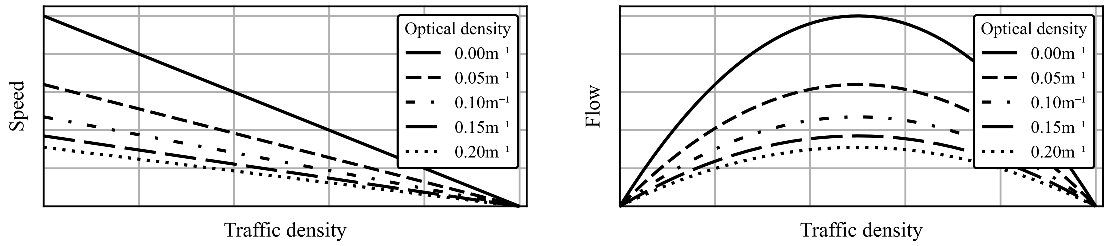


*Figure 8. Calibrated adapted Greenshield model, adapted to reduced visibility.*

### 2.4.2 Calibrated Daganzo model (1994)

The bi-linear model by Daganzo (see Equation 4) relies on three parameters: the free-flow speed, the critical density, and the jam density. The critical speed always equals the free-flow speed in this model, which means that the model imposes that $\gamma$ equals $\beta$.

The Daganzo model can be adjusted according to Equation 20, as presented in Equation 22.

$$v_{sm} = \begin{Bmatrix} \alpha\, v_f, & 0 \leq k \leq k_c \\ \alpha\, v_c \frac{k_c}{k} \frac{k_j - k}{k_j - k_c}, & k_c \leq k \leq k_j \end{Bmatrix} = \alpha v \qquad \text{[Equation 22]}$$

Figure 9 shows the calibrated model for five different visibility scenarios (expressed by optical density).

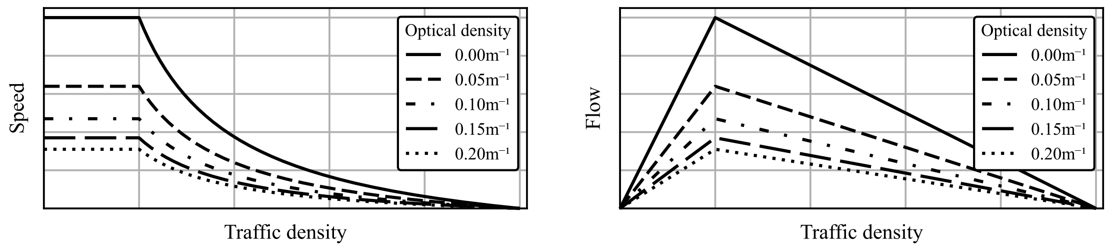


*Figure 9. Calibrated adapted Daganzo model, adapted to reduced visibility.*

### 2.4.3 Calibrated Van Aerde & Rakha (1995)

The model by Van Aerde & Rakha relies on four parameters, namely ($a, b, c, v_f$) or ($v_f$, $v_c$, $k_c$, $k_j$). Therefore, it does not require restrictive relationships between $\alpha, \beta, \gamma$ and $\delta$. The Van Aerde model can be adjusted according to Equation 20, as presented in Equation 23.

$$\begin{Bmatrix} a_{sm} = a \\ b_{sm} = b\,\alpha \\ c_{sm} = c/\alpha \end{Bmatrix} \rightarrow k = \frac{1}{a + \frac{b}{v_f - (v_{sm}/\alpha)} + c\,(v_{sm}/\alpha)} \rightarrow v_{sm} = \alpha\, v \qquad \text{[Equation 23]}$$

Figure 10 shows the calibrated model for five different visibility scenarios (expressed by optical density).

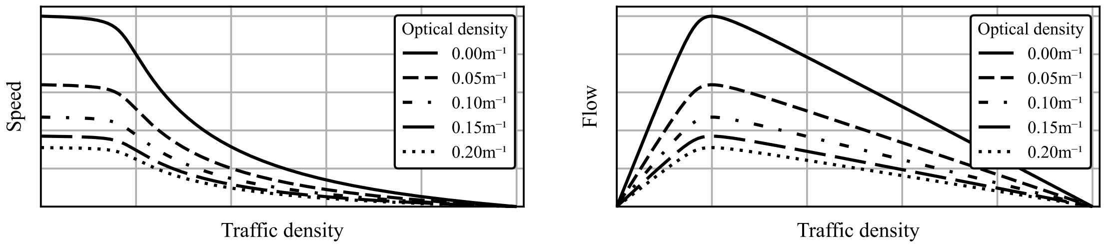


*Figure 10. Calibrated Van Aerde & Rakha model, adapted to reduced visibility.*

# 3 A conceptual framework for destination modelling considering the impact of a pandemic on shelter availability

This section introduces a conceptual framework for the representation of the decisions that take place during a wildland-urban interface fire scenario considering the impact of a pandemic scenario.

The first step is to define a possible timeline for a wildfire evacuation. This includes people who are proceeding to the evacuation to complete so before the fire reached the urbanized area. A schematic representation of this process is presented in Figure 11. The first level of the timeline represents the wildfire and its propagation. The second line refers to the actions taken by the emergency services and authorities and the third line to those by the evacuating population.

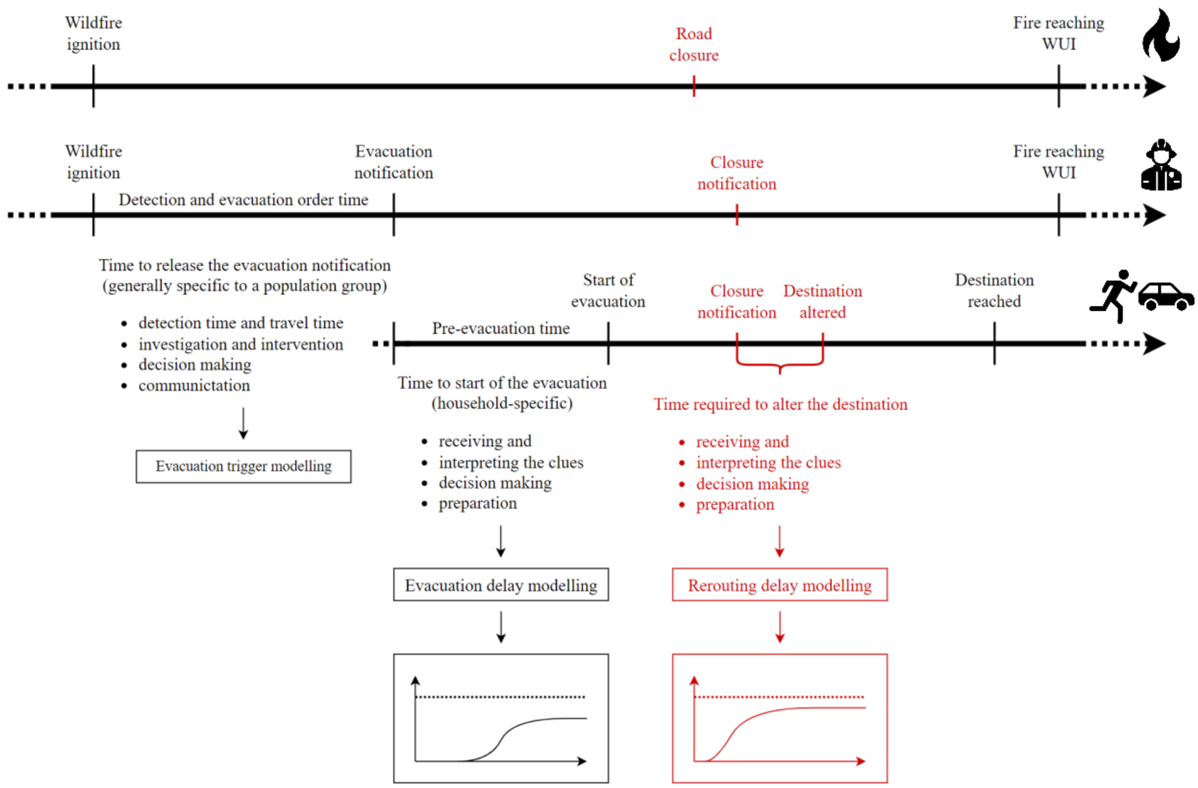


*Figure 11. Timeline of a wildfire evacuation divided into three levels (wildfire, emergency services, and population)*

In this section, the timeline at the bottom of Figure 11 is discussed. A method is proposed to model the behaviour of the evacuating population. This is represented through a flowchart, which is deemed to allow the implementation. The main effort has been placed on modelling the evacuating population considering the impact of shelter availability (e.g. due to a concurrent pandemic scenario along with a WUI fire evacuation).

Each step of this conceptual model is described in this section along with key aspects which need to be taken into consideration for the correct implementation of this modelling approach. It should be noted that this conceptual framework has been designed considering the characteristics of an integrated multi-physics model like WUI-NITY (Wahlqvist et al., 2021). Nevertheless, its implementation should be possible in other models which present comparable characteristics (i.e. they perform the representation of the key modelling layers of a WUI fire evacuation such as pedestrian response and movement, traffic evacuation and wildfire spread) and a reasonably similar level of granularity. Figure 13 presents a set of steps which are here discussed.

Start Evacuation

Here, the start of the evacuation refers to the moment at which the population receives an evacuation recommendation or an evacuation order. The start of the evacuation is either defined by the user or through a trigger buffer model, e.g., PERIL (Mitchell et al., 2022), which allows for identifying the moment at which the population should start evacuating.

Evacuation delay

The evacuation recommendation/order is followed by a reaction delay, representing the time a household spends before it starts evacuating. This includes both the time for people to become aware of the incoming threat as well as the time to respond to it (Lovreglio et al., 2016; Zhao et al., 2022). The user can define the probability distribution for the entire population or per population group. An example of such a distribution is given in Figure 12. It should be noted that those distributions may be assumed of different types (McLennan et al., 2019) and it would be beneficial for an evacuation model to allow users to customise the shape and type of the distribution in use.

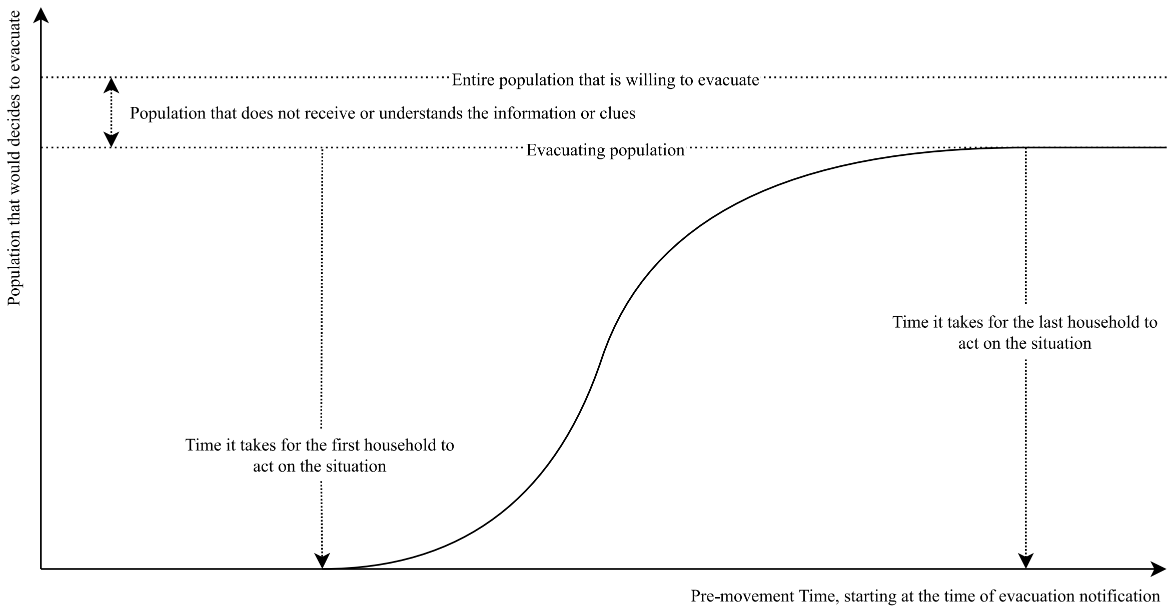


*Figure 12. Cumulative distribution of pre-evacuation time.*

Route calculations

Possible routes to be used by evacuees are pre-calculated by the evacuation simulator. These can be based on a set of assumptions which are defined either by the user or based on a given modelling approach (Bladström, 2017).

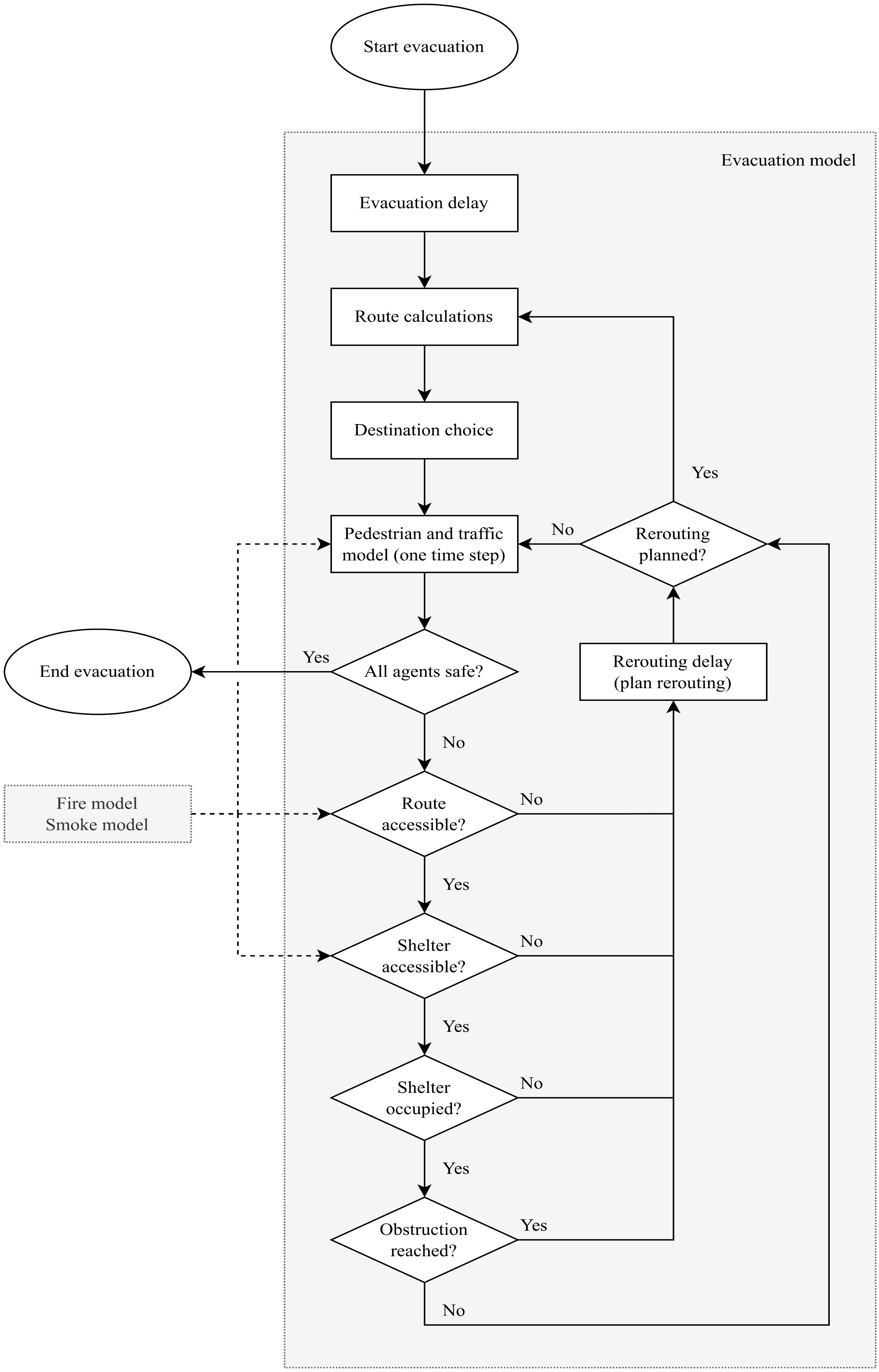


*Figure 13. Flowchart of the destination model implementation.*

Destination choice

In this step, every household is assigned a destination. The initial distribution between routes is defined by the user or based on a given approach (e.g., shorter time, shorter distance, familiar route, etc. in relation to the number of evacuees initially aiming towards a given shelter or domain exits).

Pedestrian and traffic model

Thereafter, both the pedestrian and the traffic model advance one timestep. In the pedestrian model, households are assumed to stay together. Once they reach a vehicle, decisions are made individually for each vehicle.

All agents safe?

When all agents have reached their destinations (excluding those people who decided to defend in place (McCaffrey et al., 2018; Tibbits and Whittaker, 2007)), the evacuation simulation is completed.

Route accessible?

When a given road segment is no longer accessible due to the propagation of fire and smoke or due to a traffic accident, all routes that contain that segment will be recalculated and the destination choice needs to be reconsidered. However, rerouting is unlikely to happen immediately, and a decision delay (rerouting delay) is implemented.

Shelter accessible?

The shelter accessibility is examined similarly to route accessibility. When rerouting occurs, a decision delay is implemented.

Shelter occupied?

The shelter occupation is examined. At a certain occupation level (user-defined), the shelter will be closed. Other evacuees that are still on their way to the shelter will have to reroute. Once more, this decision is taken after a certain delay.

Obstruction reached?

When a road segment or shelter closes, agents will continue to follow the original route until they have received, understood, and processed the closure notification (until the rerouting delay is over). Some evacuees might reach a fully occupied shelter, a road accident, or a fire/smoke front and therefore make faster decisions. For those agents, the planned rerouting will be performed immediately.

Rerouting delay

The rerouting delay represents the time it takes for:

- a closure to be discovered
- a notification to be released to the population
- the notification to be received and understood by the population

- a decision to be made

The user can define probability distribution for the entire population or per population group.

Rerouting planned?

After the checks are executed, the pedestrian model and traffic model can proceed with the next time step. However, if a rerouting delay ends before the next time step, then the routes and destinations of the affected vehicles must be recalculated first.

Fire model and smoke model

The fire model and smoke model run previously or simultaneously with the evacuation model and influence it on different levels. Not only can roads and shelters be closed due to the propagating fire/smoke fronts, but smoke can also influence driving behaviour (e.g. reduce driving speed or affect re-routing decisions).

# 4 Discussion

This report presented the work performed for recalibrating a set of macroscopic traffic models to include the impact of wildfire smoke on driving speed. A conceptual framework for the study of the impact of shelter availability (due to a concurrent pandemic) was also presented. This was performed to represent an evacuation condition in case of WUI fires.

An experimental relationship between smoke density and individual speed (Wetterberg et al., 2021) was adopted to recalibrate macroscopic traffic models. This was performed by implementing a set of updated speed-flow relationships considering the impact of wildfire smoke on driving speed. In fact, this report discussed previous research assessing the negative influence of rain and fog on traffic flow variables, while the influence of wildfire smoke is still largely unexplored. Smoke can affect traffic flow in different ways, especially in case of evacuations, where some links can be blocked due to the presence of smoke (Intini et al., 2019), thus dynamically affecting in turn the evacuation operations or speed increase may affect evacuation times. Compared to evacuation times in clear conditions, evacuation times can be significantly higher in case of low traffic density and low visibility conditions than in clear conditions. This means that in case of scarcely populated rural areas affected by evacuations in case of WUI fires, the effect of smoke can dramatically increase network clearance times, due to the high capacity drop due to the presence of smoke, even in presence of relatively few vehicles entering a given road section.

It should be noted that reliable real-world data concerning reduced visibility due to smoke at the drivers' height are lacking. In other words, data concerning evacuation speeds during wildfires exist (Rohaert et al., 2022; Ronchi et al., 2021), but those are not coupled with visibility conditions at the drivers' height.

The models presented here are calibrated on data collected from individual driving behaviour in smoke (Wetterberg et al., 2021). Future research should experimentally investigate how driving in smoke is affected by the concurrent presence of other vehicles and reduced visibility. In the meanwhile, it is recommended to adopt the models presented in this work, as they yield more conservative results compared to current predictions which completely omit the impact of smoke on driving speed.

An accurate estimation of evacuation time is crucial for both evacuation planning and real-time management (Chiu et al., 2007; Wolshon and Marchive, 2007). The information obtained can be applied to define trigger points/buffers (Cova et al., 2005; Mitchell et al., 2022) to define the time and/or the location at which an evacuation order should start. In addition, the evolution of fire and, consequently, smoke, can be taken into account while managing the evacuation, predicting the possible unavailability of given links due to the presence of smoke. It should be noted that the current modelling approach makes use of simplified assumptions concerning global visibility conditions in a given road link. Future work should focus on coupling such updated traffic models with a more accurate prediction of smoke spread which accounts for varying visibility during the passage of time and within a given road link.

The present work demonstrates that 1) the integration between different modelling layers is fundamental (i.e., combining fire spread models, evacuation response and traffic models) to achieve reliable predictions of evacuation clearance time; 2) such modelling layers should be able to communicate and produce credible outputs in real-time, relying on an appropriate trade-off between computational time and accuracy. For this reason, the use of the WUI-NITY platform allowing for the simulation of multiple layers affecting WUI fire evacuation (Ronchi et al. 2020; Wahlqvist et al., 2021) was selected.

Introducing the models calibrated for reduced visibility conditions in such platforms may indeed pave the way for enhanced planning and real-time management of evacuations due to wildfires in WUI areas. Clearly, this is the first attempt of filling a gap in research and practice, which surely needs further study and development. Future studies should be conducted to investigate a wider set of behaviour for different driver populations and road types, and possibly relying on data from real events (e.g. using trajectory and speed data from evacuating vehicles, e.g. making use of GPS data (Zhao et al., 2022) or traffic sensor datasets (Rohaert et al., 2022)).

In this work, simple macroscopic traffic modelling approaches were used, and this is deemed suitable for real-time management applications. This approach may need further refinement for planning purposes. In the latter case, the switch to microscopic or mesoscopic modelling can be justified (Intini et al., 2019). Moreover, the comparison between simulated evacuation and real case studies in presence of smoke from wildfires could help in assessing the validity of such an approach.

The effects of smoke on traffic evacuation are not limited to the impact on traffic flow (i.e., on travel times and congestion), but they may also cause crashes, especially during evacuation in large wildfires. Several examples of such events are reported by (Blanchi et al., 2018; McLennan et al., 2019; Toledo et al., 2018). However, while most research on wildfire evacuation cites the occurrence of traffic crashes during evacuation also due to reduced visibility conditions this aspect is still not studied from a prevention perspective.

Similarly to the recalibration of traffic models considering the impact of smoke, the conceptual framework for the representation of the impact of destination availability on evacuation is an important first step towards a more accurate prediction of evacuation times. This work is still at an initial stage and further developments will be presented within the current project

Overall, the work conducted so far demonstrated the complexities associated with WUI fire evacuation processes and paves the way towards a more accurate representation of them.

## References


Agarwal, M., Maze, T., Souleyrette, R., others, 2006. The weather and its impact on urban freeway traffic operations, in: Proceedings of the 85th Annual Meeting of the Transportation Research Board, Washington DC.

Agbolosu-Amison, S.J., Sadek, A.W., ElDessouki, W., 2004. Inclement Weather and Traffic Flow at Signalized Intersections: Case Study from Northern New England. Transportation Research Record 1867, 163–171. https://doi.org/10.3141/1867-19

Beloglazov, A., Almashor, M., Abebe, E., Richter, J., Steer, K.C.B., 2016. Simulation of wildfire evacuation with dynamic factors and model composition. Simulation Modelling Practice and Theory 60, 144–159. https://doi.org/10.1016/j.simpat.2015.10.002

Benichou, N., Adelzadeh, M., Singh, J., Gomaa, I., Elsagan, N., Kinateder, M., Ma, C., Gaur, A., Bwala, A., Sultan, M., 2021. National Guide for Wildland-urban interface fires: guidance on hazard and exposure assessment, property protection, community resilience and emergency planning to minimize the impact of wildland-urban interface fires.

Beverly, J.L., Bothwell, P., 2011. Wildfire evacuations in Canada 1980–2007. Natural Hazards 59, 571–596.

Billot, R., El Faouzi, N.-E., De Vuyst, F., 2009. Multilevel Assessment of the Impact of Rain on Drivers' Behavior: Standardized Methodology and Empirical Analysis. Transportation Research Record 2107, 134–142. https://doi.org/10.3141/2107-14

Bladström, K., 2017. Route choice modelling in fire evacuation simulators. LUTVDG/TVBB.

Blanchi, R., Whittaker, J., Haynes, K., Leonard, J., Opie, K., 2018. Surviving bushfire: the role of shelters and sheltering practices during the Black Saturday bushfires. Environmental Science & Policy 81, 86–94. https://doi.org/10.1016/j.envsci.2017.12.013

Brooks, K.R., Rafat, M.E., 2015. Simulation of driving in low-visibility conditions: Does stereopsis improve speed perception? Perception 44, 145–156.

Chiu, Y.-C., Zheng, H., Villalobos, J., Gautam, B., 2007. Modeling no-notice mass evacuation using a dynamic traffic flow optimization model. IIE Transactions 39, 83–94. https://doi.org/10.1080/07408170600946473

Colonna, P., Intini, P., Berloco, N., Ranieri, V., 2016. The influence of memory on driving behavior: How route familiarity is related to speed choice. An on-road study. Safety science 82, 456–468.

Cova, T.J., Dennison, P.E., Kim, T.H., Moritz, M.A., 2005. Setting Wildfire Evacuation Trigger Points Using Fire Spread Modeling and GIS. Transactions in GIS 9, 603–617. https://doi.org/10.1111/j.1467-9671.2005.00237.x

Daganzo, C.F., 1994. The cell transmission model: A dynamic representation of highway traffic consistent with the hydrodynamic theory. Transportation Research Part B: Methodological 28, 269–287. https://doi.org/10.1016/0191-2615(94)90002-7

Del Castillo, J.M., Benítez, F.G., 1995. On the functional form of the speed-density relationship - Part I: General theory. Transportation Research Part B: Methodological 29, 373–389. https://doi.org/10.1016/0191-2615(95)00008-2

Dennison, P.E., Cova, T.J., Mortiz, M.A., 2007. WUIVAC: a wildland-urban interface evacuation trigger model applied in strategic wildfire scenarios. Natural Hazards 41, 181–199.

Dhaliwal, S.S., Wu, X., Thai, J., Jia, X., 2017. Effects of Rain on Freeway Traffic in Southern California. Transportation Research Record 2616, 69–80. https://doi.org/10.3141/2616-08

Dixit, V., Wolshon, B., 2014. Evacuation traffic dynamics. Transportation Research Part C: Emerging Technologies 49, 114–125. https://doi.org/10.1016/J.TRC.2014.10.014

Dowling, R., Ryus, P., Schroeder, B., Kyte, M., Creasey, F.T., Rouphail, N., Hajbabaie, A., Rhoades, D., 2016. Planning and preliminary engineering applications guide to the highway capacity manual.

Drake, J., Schofer, J., May, A., 1965. A statistical analysis of speed-density hypotheses. Traffic Flow and Transportation 53–87.

Greenshield, B.D., 1935. A study of Traffic Capacity. Proceedings of the Fourteenth Annual Meeting of the Highway Research Board Held at Washington, D.C. December 6-7, 1934. Part I 14, 448–477.

Hassan, E.M., Mahmoud, H.N., 2021. Orchestrating performance of healthcare networks subjected to the compound events of natural disasters and pandemic. Nature communications 12, 1–12.

Henderson, S.B., 2020. The COVID-19 pandemic and wildfire smoke: potentially concomitant disasters. American journal of public health.

Highway capacity manual: a guide for multimodal mobility analysis, Sixth edition. ed, 2016. . Transportation Research Board, Washington, D.C.

Hoogendoorn, R., Tamminga, G., Hoogendoorn, S., Daamen, W., 2010. Longitudinal driving behavior under adverse weather conditions: Adaptation effects, model performance and freeway capacity in case of fog, in: Intelligent Transportation Systems (Itsc), 2010 13th International Ieee Conference On. IEEE, pp. 450–455.

Ibrahim, A.T., Hall, F.L., 1994. Effect of adverse weather conditions on speed-flow-occupancy relationships.

International Standards Organization, 2020. Fire Safety Engineering - Verification and validation protocol for building fire evacuation models ISO/DIS 20414.

Intini, P., Ronchi, E., Gwynne, S., Pel, A., 2019. Traffic Modeling for Wildland–Urban Interface Fire Evacuation. Journal of Transportation Engineering, Part A: Systems 145, 04019002.

Intini, P., Wahlqvist, J., Wetterberg, N., Ronchi, E., 2022. Modelling the impact of wildfire smoke on driving speed. International Journal of Disaster Risk Reduction.

Kinateder, M., Ronchi, E., Nilsson, D., Kobes, M., Müller, M., Pauli, P., Mühlberger, A., 2014. Virtual Reality for Fire Evacuation Research, in: 1st Workshop "Complex Events and Information Modelling." Warsaw, pp. 319–327.

Kolen, B., Helsloot, I., 2012. Time needed to evacuate the Netherlands in the event of large-scale flooding: strategies and consequences. Disasters 36, 700–722.

Li, D., Cova, T.J., Dennison, P.E., 2015. A household-level approach to staging wildfire evacuation warnings using trigger modeling. Computers, Environment and Urban Systems 54, 56–67.

Lighthill, M.J., Whitham, G., 1955. On kinematic waves I. Flood movement in long rivers. Proceedings of the Royal Society of London. Series A. Mathematical and Physical Sciences 229, 281–316.

Lindell, M.K., Kang, J.E., Prater, C.S., 2011. The logistics of household hurricane evacuation. Natural hazards 58, 1093–1109.

Lovreglio, R., Ronchi, E., Nilsson, D., 2016. An Evacuation Decision Model based on perceived risk, social influence and behavioural uncertainty. Simulation Modelling Practice and Theory 66, 226–242. https://doi.org/10.1016/j.simpat.2016.03.006

McCaffrey, S., Wilson, R., Konar, A., 2018. Should I stay or should I go now? Or should I wait and see? Influences on wildfire evacuation decisions. Risk analysis 38, 1390–1404.

McLennan, J., Ryan, B., Bearman, C., Toh, K., 2019. Should We Leave Now? Behavioral Factors in Evacuation Under Wildfire Threat. Fire Technology 55, 487–516. https://doi.org/10.1007/s10694-018-0753-8

Mitchell, H., Gwynne, S.M.V., Ronchi, E., Kalogeropoulos, N., Rein, G., 2022. Integrating wildfire spread and evacuation times to design safe triggers: application to two rural communities using PERIL model. Safety Science.

Rakha, H., Farzaneh, M., Arafeh, M., Hranac, R., Sterzin, E., Krechmer, D., 2007. Empirical studies on traffic flow in inclement weather. Virginia Tech Transportation Institute.

Richards, P.I., 1956. Shock waves on the highway. Operations research 4, 42–51.

Rohaert, A., Kuligowski, E., Ardinge, A., Wahlqvist, J., Gwynne, S., Kimball, A., Benichou, N., Ronchi, E., 2022. Traffic dynamics during the 2019 Kincade wildfire evacuation. [Submitted for peer-review to an international journal.].

Ronchi, E., Gwynne, S., 2019. Computational Evacuation Modeling in Wildfires, in: Manzello, S.L. (Ed.), Encyclopedia of Wildfires and Wildland-Urban Interface (WUI) Fires. Springer International Publishing, Cham, pp. 1–10. https://doi.org/10.1007/978-3-319-51727-8_121-1

Ronchi, E., Gwynne, S.M.V., Purser, D.A., Colonna, P., 2013. Representation of the Impact of Smoke on Agent Walking Speeds in Evacuation Models. Fire Technology 49, 411–431. https://doi.org/10.1007/s10694-012-0280-y

Ronchi, E., Gwynne, S.M.V., Rein, G., Intini, P., Wadhwani, R., 2019. An open multi-physics framework for modelling wildland-urban interface fire evacuations. Safety Science 118, 868–880. https://doi.org/10.1016/j.ssci.2019.06.009

Ronchi, E., Wahlqvist, J., Gwynne, S., Kinateder, M., Rein, G., Mitchell, H., Benichou, N., Ma, C., Kimball, A., 2020. WUI-NITY: a platform for the simulation of wildland-urban interface fire evacuation. Fire Protection Research Foundation, Quincy, MA (USA).

Ronchi, E., Wahlqvist, J., Rohaert, A., Ardinge, A., Gwynne, S.M.V., Rein, G., Mitchell, H., Kalogeropoulos, N., Kinateder, M., Benichou, N., Kuligowski, E., Westbury, A., Kimball, A., 2021. WUI-NITY 2: the integration, verification, and validation of the wildfire evacuation platform WUI-NITY. Fire Protection Research Foundation, Quincy, MA (USA).

Smith, B.L., Byrne, K.G., Copperman, R.B., Hennessy, S.M., Goodall, N.J., 2004. An investigation into the impact of rainfall on freeway traffic flow, in: 83rd Annual Meeting of the Transportation Research Board, Washington DC. Citeseer.

Snowden, R.J., Stimpson, N., Ruddle, R.A., 1998. Speed perception fogs up as visibility drops. Nature 392, 450.

Sugg, M.M., Runkle, J.D., Hajnos, S.N., Green, S., Michael, K.D., 2022. Understanding the concurrent risk of mental health and dangerous wildfire events in the COVID-19 pandemic. Science of the total environment 806, 150391.

Sullivan, J., Novak, D., Aultman-Hall, L., Scott, D.M., 2010. Identifying critical road segments and measuring system-wide robustness in transportation networks with isolating links: A link-based capacity-reduction approach. Transportation Research Part A: Policy and Practice 44, 323–336.

Tibbits, A., Whittaker, J., 2007. Stay and defend or leave early: policy problems and experiences during the 2003 Victorian bushfires. Environmental Hazards 7, 283–290.

Tohidi, A., 2016. Experimental and Numerical Modeling of Wildfire Spread via Fire Spotting. Clemson University.

Toledo, T., Marom, I., Grimberg, E., Bekhor, S., 2018. Analysis of evacuation behavior in a wildfire event. International Journal of Disaster Risk Reduction 31, 1366–1373. https://doi.org/10.1016/j.ijdrr.2018.03.033

Transportation Research Board, National Research Council, 2016. Chapter 12: Basic Freeway and Multilane Highway Segments, in: Elefteriadou, L.A. (Ed.), Highway Capacity Manual 6th Edition: A Guide for Multimodal Mobility Analysis. National Academies Press, Washington, D.C., p. 12.1-12.62. https://doi.org/10.17226/24798

Underwood, R.T., 1961. Speed, volume and density relationships. Quality and Theory of Traffic Flow. A Symposium, Yale University Bureau of Highway Traffic 141–188.

Van Aerde, M., Rakha, H., 1995. Multivariate calibration of single regime speed-flow-density relationships. Presented at the Pacific Rim TransTech Conference. 1995 Vehicle Navigation and Information Systems Conference Proceedings. 6th International VNIS. A Ride into the Future, IEEE, pp. 334–341. https://doi.org/10.1109/VNIS.1995.518858

Wahlqvist, J., Ronchi, E., Gwynne, S.M.V., Kinateder, M., Rein, G., Mitchell, H., Bénichou, N., Ma, C., Kimball, A., Kuligowski, E., 2021. The simulation of wildland-urban interface fire evacuation: The WUI-NITY platform. Safety Science 136, 105145. https://doi.org/10.1016/j.ssci.2020.105145

Westhaver, A., 2017. Why some homes survived: Learning from the Fort McMurray wildland/urban interface fire disaster.

Wetterberg, N., Ronchi, E., Wahlqvist, J., 2021. Individual Driving Behaviour in Wildfire Smoke. Fire Technology 57, 1041–1061.

Wilmot, C.G., Mei, B., 2004. Comparison of alternative trip generation models for hurricane evacuation. Natural hazards review 5, 170–178.

Wolshon, B., 2001. "one-way-out": contraflow freeway operation for hurricane evacuation. Natural hazards review 2, 105–112.

Wolshon, B., Marchive, E., 2007. Emergency Planning in the Urban-Wildland Interface: Subdivision-Level Analysis of Wildfire Evacuations. Journal of Urban Planning and Development 133, 73–81. https://doi.org/10.1061/(ASCE)0733-9488(2007)133:1(73)

Wong, S., Broader, J., Shaheen, S.A., 2020. Review of California Wildfire Evacuations from 2017 to 2019. University of California, Institute of Transportation Studies, ITS Reports. https://doi.org/10.7922/G29G5K2R

Wong, S.D., Pel, A.J., Shaheen, S.A., Chorus, C.G., 2020. Fleeing from hurricane Irma: Empirical analysis of evacuation behavior using discrete choice theory. Transportation Research Part D: Transport and Environment 79, 102227.

Wu, N., Rakha, H., 2009. Derivation of Van Aerde Traffic Stream Model from Tandem-Queuing Theory. Transportation Research Record: Journal of the Transportation Research Board 2124, 18–27. https://doi.org/10.3141/2124-02

Zhao, X., Xu, Y., Lovreglio, R., Kuligowski, E., Nilsson, D., Cova, T.J., Wu, A., Yan, X., 2022. Estimating wildfire evacuation decision and departure timing using large-scale GPS data. Transportation Research Part D: Transport and Environment 107, 103277. https://doi.org/10.1016/j.trd.2022.103277